

17. Coating: Dynamic Contact Lines

Last time we considered the Landau-Levich-Derjaguin Problem and deduced

$$h \sim \ell_c Ca^{2/3} \text{ for } Ca = \frac{\mu V}{\sigma} < 10^{-3}$$

$$h \sim \ell_c Ca^{1/3} \text{ for } Ca \rightarrow 1.$$

The influence of surfactants

Surfactants decrease σ which affects h slightly. But the principle effect is to generate Marangoni stresses that increase fluid emplacement: h typically doubles.

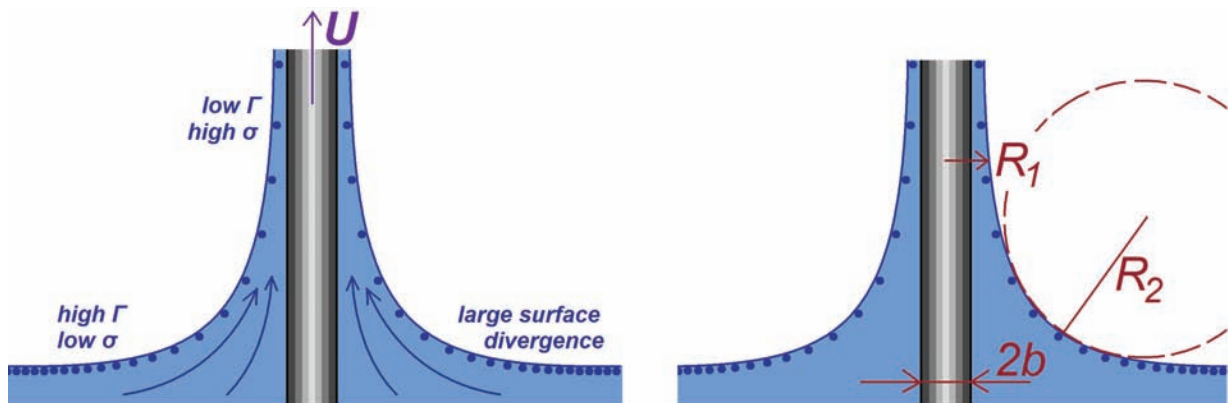


Figure 17.1: The influence of surfactants on fiber coating. Gradients in Γ induce Marangoni stresses that enhance deposition.

Fiber coating:

$$\text{Normal stress: } p_0 + \sigma \left(\frac{1}{R_1} + \frac{1}{R_2} \right) = p_0 - \rho g z.$$

If $b \ll \ell_c$, $\frac{1}{R_1} \sim \frac{1}{b} \Rightarrow$ curvature pressures dominant, can't be balanced by gravity.

Thus, the interface must take the form of a catenoid: $\frac{1}{R_1} + \frac{1}{R_2} = 0$.

For wetting, $\theta_e = 0 \Rightarrow r(z) = b \cosh\left(\frac{z-h}{b}\right)$ where $h \approx b \ln(2\ell_c/b)$.

Note:

1. gravity prevents meniscus from extending to $\infty \Rightarrow h$ deduced by cutting it off at ℓ_c .
2. h is just a few times b ($h \ll \ell_c$) \Rightarrow lateral extent greatly exceeds its height.

Forced wetting on fibers e.g. optical fiber coating.

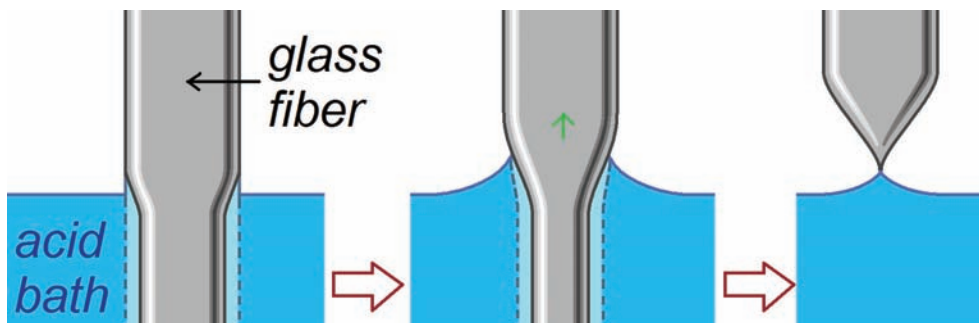


Figure 17.2: Etching of the microtips of Atomic Force Microscopes. As the fiber is withdrawn from the acid bath, the meniscus retreats and a sharp tip forms.

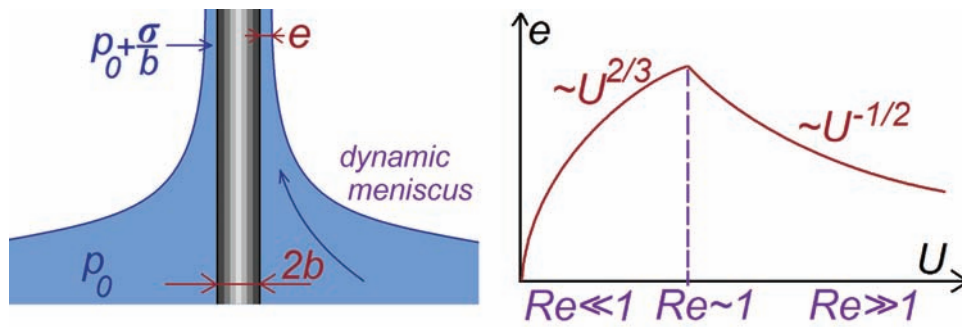


Figure 17.3: *Left*: Forced wetting on a fiber. *Right*: The coating thickness as a function of the Reynolds number Re .

$p_{film} \sim p_0 + \frac{\sigma}{b}$, $p_{meniscus} \sim p_0 \Rightarrow \Delta p \sim \frac{\sigma}{b}$ resists entrainment.

Force balance: $\mu \frac{U}{e^2} \sim \frac{\Delta p}{L} = \frac{\sigma}{bL}$.

Pressure match: $\frac{e}{L^2} \sim \frac{1}{b} \Rightarrow L \sim \sqrt{be}$, substitute into the previous equation to find

$$e \approx bCa^{2/3} \quad (\text{Bretherton's Law}) \quad (17.1)$$

Note:

- this scaling is valid when $e \ll b$, i.e. $Ca^{2/3} \ll 1$.
- At higher Ca , film is the viscous boundary layer that develops during pulling: $\delta \sim \left(\frac{\mu}{\rho} \frac{L_s}{U}\right)^{1/2}$, where L_s is the submerged length.

Displacement of an interface in a tube

E.g. air evacuating a water-filled pipette, pumping oil out of rock with water.

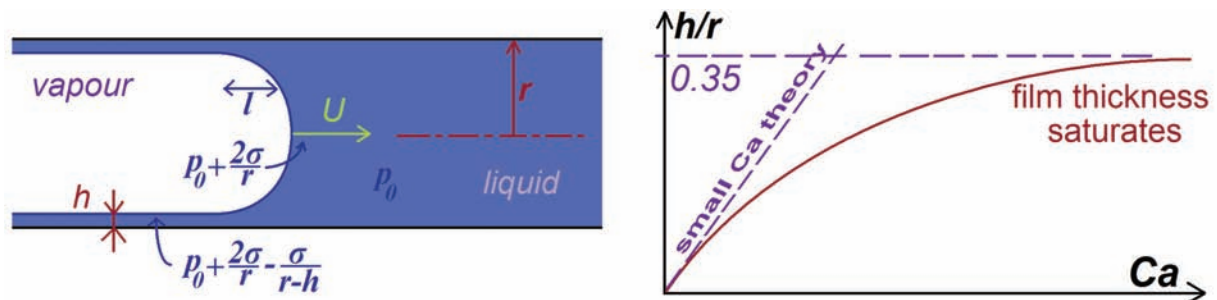


Figure 17.4: *Left*: Displacing a liquid with a vapour in a tube. *Right*: The dependence of the film thickness left by the intruding front as a function of $Ca = \mu U / \sigma$.

In the limit of $h \ll r$, the pressure gradient in the meniscus $\nabla p \sim \frac{\sigma}{rl}$, where l is the extent of the dynamic meniscus.

As on a fiber, pressure matching: $p_0 + \frac{2\sigma}{r} - \frac{\sigma}{r-h} \sim p_0 + \frac{\sigma h}{l^2} \Rightarrow l \sim (hr)^{1/2}$ when $h \ll r$.

Force balance: $\underbrace{\mu U / h^2}_{\text{viscous}} \sim \underbrace{\sigma / rl}_{\text{curvature}} \sim \sigma / r(hr)^{1/2} \Rightarrow$

$$h \sim rCa^{2/3} \quad (\text{Bretherton 1961}) \quad (17.2)$$

where $Ca = \frac{\mu U}{\sigma}$.

Thick films: what if $h = \text{ord}(r)$? For $h \sim r$, Taylor (1961) found $h \sim (r-h)Ca^{2/3}$.

17.1 Contact Line Dynamics

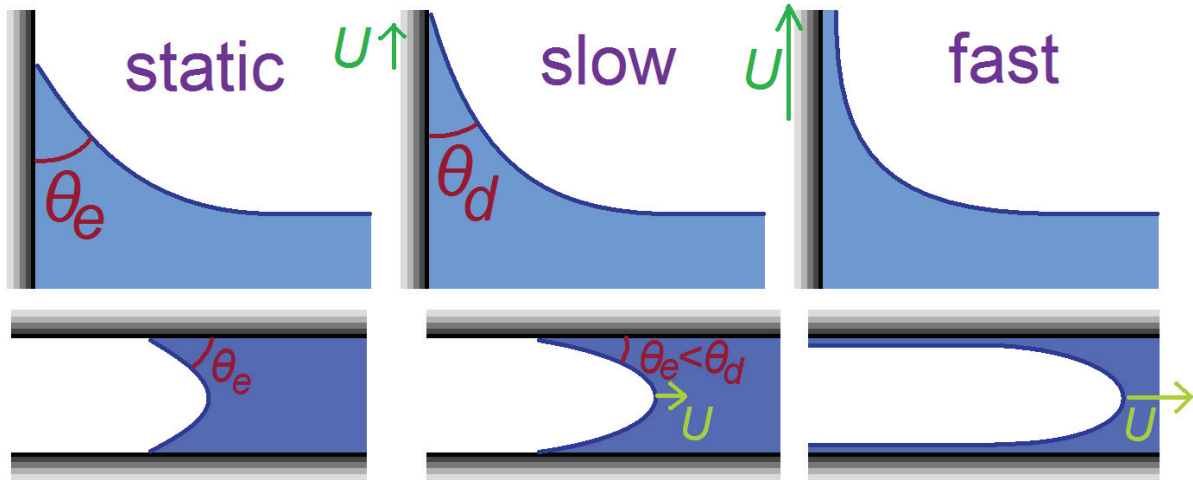


Figure 17.5: The form of a moving meniscus near a wall or inside a tube for three different speeds.

We consider the withdrawal of a plate from a fluid bath (Fig. 16.6) or fluid displacement within a cylindrical tube. **Observations:**

- at low speeds, the contact line advances at the dynamic contact angle $\theta_d < \theta_e$
- dynamic contact angle θ_d decreases progressively as U increases until $U = U_M$.
- at sufficiently high speed, the contact line cannot keep up with the imposed speed and a film is entrained onto the solid.

Now consider a clean system free of hysteresis.

Force of traction pulling liquid towards a dry region:

$$F(\theta_d) = \gamma_{SV} - \gamma_{SL} - \gamma \cos \theta_d.$$

Note:

- $F(\theta_e) = 0$ in equilibrium. How does F depend on U ? What is $\theta_d(U)$?
- the retreating contact line ($F < 0$) was examined with retraction experiments e.g. plate withdrawal.
- the advancing contact line ($F > 0$) was examined by *Hoffmann (1975)* for the case of $\theta_e = 0$.
- he found $\theta_d \sim U^{1/3} \sim Ca^{1/3}$ (Tanner's Law)

Dussan (1979): drop in vicinity of contact line advances like a tractor tread

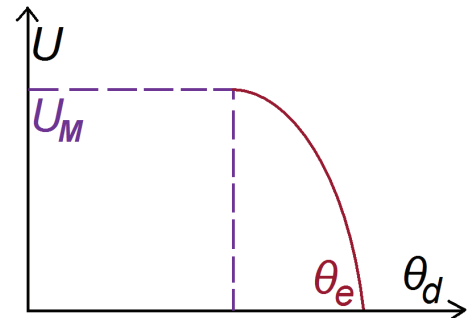


Figure 17.6: Dynamic contact angle θ_d as a function of the differential speed U . For $U > U_M$, the fluid wets the solid.

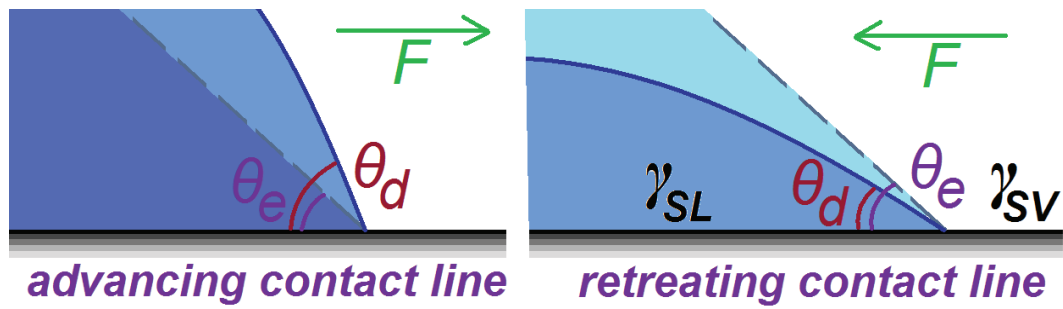


Figure 17.7: The advancing and retreating contact angles of a drop.

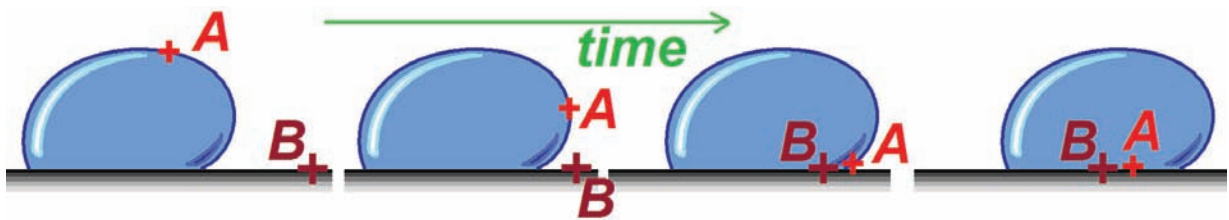


Figure 17.8: A drop advancing over a solid boundary behaves like a tractor tread (Dussan 1979), advancing through a rolling motion.

Flow near advancing contact line

We now consider the flow near the contact line of a spreading liquid ($\theta_d > \theta_e$):

- consider $\theta_d \ll 1$, so that slope $\tan \theta_d = \frac{z}{x} \approx \theta_d \Rightarrow z \approx \theta_d x$.
- velocity gradient: $\frac{dU}{dz} \approx \frac{U}{\theta_d x}$
- rate of viscous dissipation in the corner

$$\Phi = \int \int_{corner} \mu \left(\frac{dv}{dz} \right)^2 dU = \mu \int_0^\infty dx \int_0^{z_{max}=\theta_d x} \frac{U^2}{\theta_d^2 x^2} dz \tag{17.3}$$

$$\Phi = 3\mu \int_0^\infty \frac{U^2}{\theta_d^2 x^2} \theta_d x dx = \frac{3\mu U^2}{\theta_d} \int_0^\infty \frac{dx}{x} \tag{17.4}$$

de Gennes' approximation: $\int_0^\infty \frac{dx}{x} \approx \int_a^L \frac{dx}{x} = \ln L/a \equiv \ell_D$

where L is the drop size and a is the molecular size. From experiments $15 < \ell_D < 20$.

Energetics:

$$FU = \Phi = \frac{3\mu \ell_D}{\theta_d} \cdot U^2 \tag{17.5}$$

rate of work done by surface forces equals the rate of viscous dissipation.

Recall:

- $F = \gamma_{SV} - \gamma_{SL} - \gamma \cos \theta_d = \gamma (\cos \theta_e - \cos \theta_d)$
- in the limit $\theta_e < \theta_d \ll 1$, $\cos \theta \approx 1 - \frac{\theta^2}{2} \Rightarrow F \approx \frac{\gamma}{2} (\theta_d^2 - \theta_e^2)$
- substitute F into the energetics equation to get the contact line speed:

$$U = \frac{U^*}{6\ell_D} \theta_d (\theta_d^2 - \theta_e^2) \tag{17.6}$$

where $U^* = \frac{\gamma}{\mu} \approx 30\text{m/s}$.

Note:

1. rationalizes Hoffmann's data (obtained for $\theta_e = 0$) $\Rightarrow U \sim \theta_D^3$
2. $U = 0$ for $\theta_d = \theta_e$ (static equilibrium)
3. $U = 0$ as $\theta_d \rightarrow 0$: dissipation in sharp wedge impedes motion.
4. $U(\theta_d)$ has a maximum when $\frac{dU}{d\theta_d} = \frac{U^*}{6\ell_D} (3\theta_d^2 - \theta_e^2) \Rightarrow \theta_d = \frac{\theta_e}{\sqrt{3}} \Rightarrow U_{max} = \frac{U^*}{9\sqrt{3}\ell_D} \theta_e^3$

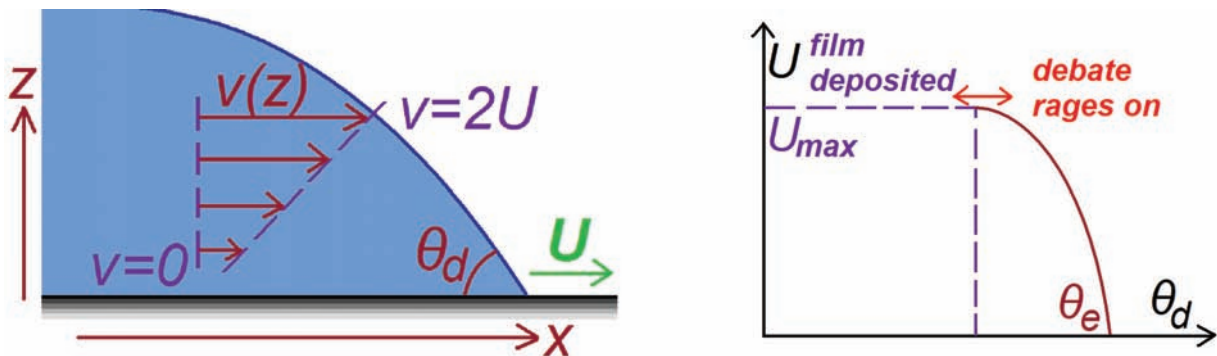


Figure 17.9: *Left*: Schematic illustration of the flow in the vicinity of an advancing contact line. *Right*: The dependence of the dynamic contact angle on the speed of withdrawal.

E.g. In water, $U^* = 70\text{m/s}$. With $\theta_e = 0.1$ radians and $\ell_D = 20$, $U_{max} = 0.2\text{mm/s}$
 \Rightarrow sets upper bound on extraction speed for water coating flows.

MIT OpenCourseWare
<http://ocw.mit.edu>

357 Interfacial Phenomena
Fall 2010

For information about citing these materials or our Terms of Use, visit: <http://ocw.mit.edu/terms>.